

## Detecting nonlinear oscillations in broadband signals

Martin Vejmelka<sup>a)</sup> and Milan Paluš

*Institute of Computer Science, Academy of Sciences of the Czech Republic,  
Pod vodárenskou věží 2, 182 07 Prague 8, Czech Republic*

(Received 5 December 2008; accepted 6 February 2009; published online 31 March 2009)

A framework for detecting nonlinear oscillatory activity in broadband time series is presented. First, a narrow-band oscillatory mode is extracted from a broadband background. Second, it is tested whether the extracted mode is significantly different from linearly filtered noise, modeled as a linear stochastic process possibly passed through a static nonlinear transformation. If a nonlinear oscillatory mode is positively detected, it can be further analyzed using nonlinear approaches such as phase synchronization analysis. For linear processes standard approaches, such as the coherence analysis, are more appropriate. The method is illustrated in a numerical example and applied to analyze experimentally obtained human electroencephalogram time series from a sleeping subject.

© 2009 American Institute of Physics. [DOI: 10.1063/1.3089880]

**Many recent scientific efforts focus on the importance of oscillatory activity in biological and physical systems especially in the context of phase dynamics and phase synchronization. For instance, oscillations in various frequency bands of the electroencephalogram have become important in understanding the function of the central nervous system. Typical approaches to analyzing data involve applying Fourier decomposition, wavelet transform, or the newer empirical mode decomposition to a time series to extract a set of modes or time series confined within a certain frequency band. These methods themselves, however, do not address the question of what character is the content of the extracted mode. In order to satisfy further data processing based on nonlinear approaches such as phase synchronization analysis, one should provide sufficient evidence that the obtained signal can be interpreted as oscillatory activity of a self-sustained, nonlinear dynamical system.**

### I. INTRODUCTION

The search for repetitive patterns in erratic, seemingly random dynamical behavior is an important way how to understand, model, and predict complex phenomena. Cyclic, oscillatory phenomena are sought in complex dynamics observed in diverse fields from physics and technology, through meteorology and climatology to neurophysiology. In cortical networks, oscillatory phenomena are observed which span five orders of magnitude in frequency.<sup>1</sup> These oscillations are phylogenetically preserved, suggesting that they are functionally relevant. Among the well-known neural oscillatory phenomena, the  $\delta$ -,  $\theta$ -,  $\alpha$ -,  $\beta$ -, and  $\gamma$ -waves can be observed in the scalp electroencephalogram (EEG). The EEG is a record of the oscillations of brain electric potentials registered from electrodes attached to the human scalp, revealing synaptic action that is moderately to strongly correlated with brain states. Oscillatory phenomena in the brain electrical

activity and their synchronization are related to cognitive processes<sup>2</sup> and their dynamical and synchronization properties change under cognitive disorders such as schizophrenia,<sup>3</sup> Alzheimer's disease, bipolar disorder, or attention-deficit hyperactivity disorder.<sup>4</sup> It is understandable that the detection and characterization of oscillatory phenomena in the brain activity are subjects of intensive research.

Besides Fourier spectral analysis, typical approaches to study brain waves involve applying wavelet decomposition or, more recently, empirical mode decomposition (EMD) and other filtering techniques to a time series to extract a set of modes or time series which contain a part of the original signal confined within a certain frequency band. The extraction parameters such as frequency or bandwidth are set by the investigator based on the position and shape of a distinct peak in the spectrum of the analyzed time series. In neuroscience the extracted narrow-band modes are often further analyzed using modern nonlinear methods, such as synchronization analysis, in order to infer possible cooperative behavior of distant parts of the human brain. For phase synchronization<sup>5</sup> or directionality (causality)<sup>6</sup> analyses, the oscillatory modes are used to compute the so-called instantaneous phase, a characteristic variable of self-sustained, nonlinear oscillatory dynamical systems. Numerically, the phase can be computed from any oscillatory-type activity but its physical meaning is unclear. Thus it is desirable to provide arguments that the observed oscillatory phenomena come from self-sustained nonlinear dynamical systems in order to avoid applications of nonlinear approaches to linearly filtered noise.

Some previous works exist which try to examine candidate modes of the investigated time series. Intricate procedures such as singular spectrum analysis (SSA), used especially in the field of climatology and meteorology,<sup>7</sup> perform a principal component analysis in the time domain. Monte Carlo SSA (Ref. 8) tests the existence of oscillatory modes by computing the variance (energy content) of each mode and verifying if it is outside the expected range for a particular background process, such as a red noise process. Re-

<sup>a)</sup>Electronic mail: vejmelka@cs.cas.cz.

cently, the method has been modified to test the dynamics of the candidate mode.<sup>9,10</sup> These methods prescribe a particular way in which the candidate modes are extracted and tested.

In this work a method is proposed which is able to detect weak oscillatory signals with dynamics different from that of filtered noise and which is effectively independent of the way how the candidate mode is obtained.

The paper continues with a description of the detection methods in Sec. II, with results obtained in numerical experiments and on actual data in Sec. III, and finishes with a discussion and conclusion in Sec. IV.

## II. METHODS

Important parts of the proposed method are the procedure to generate the surrogate time series, the mathematical objects that statistically capture required properties of analyzed time series, and the function which quantifies the difference between the dynamical structures of two time series, namely, the original and the surrogate one. Here surrogate time series are constructed so that their linear structure (autocorrelation structure) matches that of the analyzed data. If at the same time the nonlinear structure of the data significantly deviates from that of the surrogate time series, then it is inferred that a nonlinear process is involved in the generation of the data. Multiple surrogate generation algorithms exist, but each method typically has some shortcoming which may call into question the validity of the proposed method. The purpose of the test of coincidence of linear structures is to explicitly verify that the surrogate time series approximate the linear properties of the analyzed time series sufficiently well.

The data are first preprocessed by an amplitude adjustment procedure which ensures that the sample distribution of the analyzed data segment is Gaussian. The samples in the time series are ranked and an equally sized normally distributed set of samples is created. The time series samples are replaced with samples of equal rank from the normally distributed set. This step ensures that the influence of any bijective nonlinear measurement function is excluded from the test for nonlinear structure. The original unadjusted (filtered) time series data are not used henceforth and any reference to the extracted mode refers to the amplitude-adjusted version.

The surrogate data set is generated by repeated runs of an autoregressive model that has been fitted to the extracted mode. An autoregressive (AR) model is powerful enough to represent any type of filtered noise. However, in the context of detecting nonlinear dynamics, Fourier transform (FT)-based surrogate data<sup>11</sup> and their more elaborated versions such as amplitude-adjusted (AAFT) and iterated AAFT (IAFT) surrogate data<sup>12</sup> have been used more frequently. The nonlinearity tests with the FT surrogate data tend to have higher sensitivity than the tests with the AR surrogate data,<sup>13</sup> however, at the cost of lower specificity, i.e., the higher counts of false positive outcomes. Kugiumtzis<sup>14</sup> showed that surrogate data from a transformed AR model give more consistent results than the AAFT and IAFT surrogate data. The latter results have been confirmed in our experiments, and considering also the experience that the FT surrogate data are

problematic when analyzing oscillatory data,<sup>15,16</sup> we opted for the AR model surrogate data.

An AR model of order  $K$  is specified as

$$x(t) = \sum_{i=1}^K a_i x(t-i) + \mu + \sigma \xi(t), \quad (1)$$

where  $a_i$  are the coefficients of the model,  $\mu$  is the mean of the generated time series, and  $\sigma$  is the standard deviation of the uncorrelated Gaussian noise term  $\xi(t)$ . The optimal order of the autoregressive model is unknown and a model selection method must be employed. Here the Bayesian information criterion<sup>17</sup> (BIC) is used. The BIC is given by

$$\text{BIC}(K) = N \log \left( \frac{1}{N} \sum_{i=1}^N \epsilon(i)^2 \right) + (K+2) \log N, \quad (2)$$

where  $\epsilon(i)$  are the residuals of the best model fit to the original time series and  $N$  is the number of points in the time series. The number of free parameters of the estimation is  $K+2$  as besides the  $K$  model coefficients also the mean value, and the standard deviation of the input noise is estimated from the same data set. A maximum admissible order is specified before the fitting procedure begins and models of all smaller orders are fitted using least squares to the time series. The BIC is computed for each fitted model and the model with the smallest BIC value is selected. Surrogate data are generated by randomly shuffling the residuals of the fit and feeding them back into the identified model as the source noise. Using this procedure an arbitrary amount of surrogate time series can be generated.

The linear structure of a time series is characterized by linear regularity or predictability measure which is based on the linear version of time delayed mutual information (“linear redundancy”<sup>16</sup>),

$$I_{\text{lin}}(X; X_\tau) = -\frac{1}{2} \log(1 - \rho_\tau^2), \quad (3)$$

where  $\rho_\tau$  is the correlation coefficient of the time series of process  $X$  and a version of itself shifted by  $\tau$  samples  $X_\tau$ . If the autoregressive model replicates the linear properties of the analyzed data accurately, then the sequence  $I_{\text{lin}}(X; X_\tau)$  for  $\tau \in \{1, 2, \dots, \tau_{\text{max}}\}$  will agree with the corresponding linear regularity from the surrogates. Clearly the maximum lag  $\tau_{\text{max}}$  for which the shapes of the linear redundancy sequence coincide with the surrogates must be limited as the autoregressive model is only a fitted approximation of the underlying generating system. For further analysis a  $\tau_{\text{max}}$  should be selected such that linear regularity is well matched between the data and the surrogate set. A quantitative test of the agreement of the sequences is a part of the method. However, visual examination of the curves is encouraged as this can reveal problems discussed later in the paper such as inadequate sampling rate.

The nonlinear structure is captured by nonlinear regularity<sup>16</sup> which is defined analogically to linear regularity. Nonlinear regularity is based on mutual information between a time series and its shifted version. In this work equiquantal binning is first applied to assign the time series samples to a

discrete set of bins  $\xi \in \Xi$ . Mutual information, also called redundancy or nonlinear redundancy, may then be estimated as

$$I(X;X_\tau) = \sum_{\xi_1, \xi_2 \in \Xi} p(\xi_1, \xi_2) \log \frac{p(\xi_1, \xi_2)}{p(\xi_1)p(\xi_2)}, \quad (4)$$

where  $p(\xi_1)$  is the probability with which the symbol  $\xi_1$  appears in the time series and  $p(\xi_1, \xi_2)$  is the estimated probability that symbols  $\xi_1$  and  $\xi_2$  occur at the same point in the original and shifted version of the time series. The mutual information obtained using the equiquantal estimator is invariant with respect to bijective nonlinear transformations.<sup>18</sup>

A function that estimates the similarity of two sequences is necessary to compare the linear and nonlinear structures of time series. A signed version of the  $l_2$  metric,

$$l_2^\pm(x(n), y(n)) = \frac{1}{\tau_{\max}} \sum_{i=1}^{\tau_{\max}} \text{sgn}(x(i) - y(i))(x(i) - y(i))^2, \quad (5)$$

where  $\tau_{\max}$  is the maximum lag, is used to quantitatively estimate how much two sequences match. The sign of  $l_2^\pm(\cdot, \cdot)$  is positive if the first sequence lies mainly above the second sequence and negative if the opposite is true. If the points of the sequences are close together, then the absolute value of the function is close to zero. If the second sequence  $y(n)$  is fixed, then the function has only one free parameter  $x(n)$  and computes how close the given sequence is to the reference sequence  $y(n)$ .

The method proceeds by performing two hypothesis tests. The first test checks if the linear structure of the surrogates matches that of the data and the second does the same for the nonlinear structure. Each test is prepared in an identical fashion: the regularities are computed for lags  $\tau \in \{1, 2, \dots, \tau_{\max}\}$  for the data time series and for a chosen number of surrogate time series. A reference sequence  $m(n)$  is constructed by averaging all the regularity sequences from the surrogate time series. This reference sequence is set as the second argument of Eq. (5). A set of indices may now be computed using the function  $l_2^\pm(\cdot, m(n))$  for each regularity sequence of the surrogate time series and for the data. Note that the above is done separately for linear and nonlinear regularities.

In the test for the match of linear structures, a two-sided hypothesis test is constructed which will indicate if the index  $l_2^\pm(x(n), m(n))$  computed on the data significantly deviates from the distribution of the same index on the surrogates. For the test at a nominal significance level  $\alpha$ , it is checked if

$$l_2^\pm(x(n), m(n)) < q_{\alpha/2}$$

or

$$l_2^\pm(x(n), m(n)) > q_{1-\alpha/2}, \quad (6)$$

where  $x(n)$  is the linear regularity sequence of the original data and  $q_\beta$  is the  $\beta$  quantile of the distribution of  $l_2^\pm(\cdot, m(n))$  estimated from the surrogate linear regularity sequences. A two-sided test ensures that the linear regularity of the data does not significantly deviate in either direction, above or below, from the mean of the linear regularity sequence of the surrogate time series.

The purpose of the nonlinear structure test is to verify whether the nonlinear regularity sequence computed from the original data is significantly greater than the mean nonlinear regularity sequence computed from the surrogate time series. The test statistic is again the  $l_2^\pm(\cdot, m(n))$ , where the reference sequence  $m(n)$  is the mean of the nonlinear regularity sequences from the surrogate time series. The test can be denoted as

$$l_2^\pm(x(n), m(n)) > q_{1-\alpha}, \quad (7)$$

where  $x(n)$  is the nonlinear regularity sequence of the original data and  $q_\beta$  is the  $\beta$  quantile of the distribution of  $l_2^\pm(\cdot, m(n))$  estimated from the surrogate nonlinear regularity sequences. The test is one sided as only time series the regularity of which is higher than that of the surrogates are of interest. These time series exhibit a higher amount of regularity than filtered noise.

In the case of a broadband signal, no constraint is placed on the extraction procedure of a candidate narrow-band mode. Simple bandpass filtering (Butterworth fourth order zero phase shift filtering) is used in the numerical example and in the analysis of experimentally obtained EEG data. Wavelet extraction, empirical mode EMD, or SSA-based decomposition can be applied equally well.

### III. RESULTS

In this section the method is first tested on a synthetic data set and then it is applied to sleep EEG data from a test subject measured over two nights. The results are compared to the changes in relative power in the analyzed frequency band.

#### A. Numerical example

In the numerical example it is shown how nonlinear oscillatory dynamics of the Lorenz system (which does not produce any peak in the power spectrum) is detected in a mixture with an autoregressive process. The Lorenz system is a chaotic nonlinear dynamical system exhibiting complex behavior and is given by the equations

$$\dot{x} = \sigma(y - x), \quad \dot{y} = x(\rho - z) - y, \quad \dot{z} = xy - \beta z, \quad (8)$$

where  $\sigma=10$  is the Prandtl number,  $\rho=28$  is the Rayleigh number, and  $\beta=8/3$ . The differential equations were integrated with the fourth order Runge–Kutta scheme with a timestep of  $dt=0.005$  and subsampled by a factor of 10. The Lorenz  $x$ -coordinate time series was added to a linear background noise time series represented by the following AR(5) process (also normalized to unit variance):

$$x(t) = 0.4x(t-1) - 0.05x(t-2) - 0.1x(t-3) - 0.01x(t-4) + 0.6x(t-5) + 0.6\xi(t), \quad (9)$$

where  $\xi(t)$  is a white normally distributed noise input. The above AR(5) process was created to have a gentle peak next to the frequency band of the Lorenz process activity. The frequency band including the Lorenz activity (0–1.0, cf. Fig. 2) will serve as a sensitivity test, whereas the gentle peak of the AR(5) process (located at frequency of  $\approx 1.7$ , cf. Fig. 2)

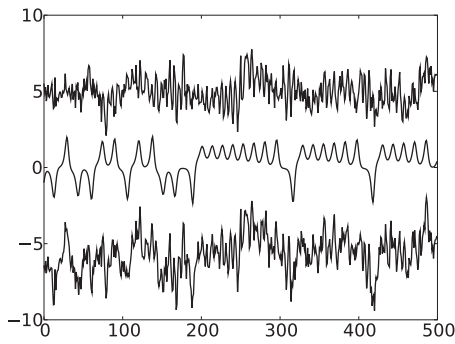


FIG. 1. A sample of the analyzed time series. The curves from top to bottom: the AR(5) process, the  $x$ -coordinate of the Lorenz oscillator, and the mixed signal. The Lorenz signal is not introducing any clear oscillatory activity into the linear autoregressive process at the given time scale. Signals have been shifted for clarity.

resulting from autoregressive filtering of white noise will serve as a specificity test.

A sample of the analyzed time series is shown in Fig. 1. The Lorenz system has not introduced a clear oscillatory activity into the autoregressive process. The spectrum of the time series estimated using the Welch periodogram method is shown in Fig. 2.

Its examination confirms that no clear oscillatory peaks have arisen through the mixing process although significant power has been added by the Lorenz oscillator to lower frequencies. In the following analysis the low frequency region of 0.05–1.05 is tested and the dominant peak in the frequency region of 1.2–2.2 is tested as a control. The mode extraction was accomplished using simple bandpass filtering with a second order Butterworth filter (forward/backward strategy equivalent to a fourth order filter with zero phase shift).

Surrogate data were constructed by fitting an autoregressive model the filtered mode with adjusted amplitudes. The order of the fitted autoregressive model fluctuated around 16 (models not shown here). The surrogate data set consisted of 200 realizations of the fitted autoregressive process constructed by shuffling the residuals and feeding them into the model as inputs. For each maximum lag from 2 to 60, 200 repetitions of the experiment were performed with newly

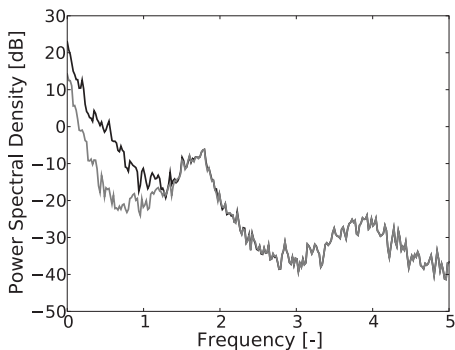


FIG. 2. Spectrum of AR(5) process (gray line) and of the AR(5) process with the Lorenz oscillator activity added (black line). The curves agree beyond frequency of  $\approx 1.5$ . Although the Lorenz oscillator adds broadband power in the lower frequencies, no clear oscillatory peak can be identified in the spectrum.

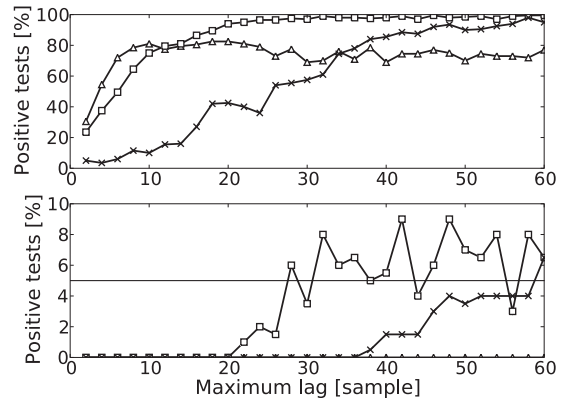


FIG. 3. Detection rates of nonlinear Lorenz activity in an AR(5) process (cf. Figs. 1 and 2) obtained from 200 realizations for different sampling rates: triangles represent detections for 5 points/period, squares for 10 points/period, and crosses for 20 points/period. Positive tests from the nonlinear redundancy statistic (top): at 5 points/period, the detection rate does not exceed 80%, with 10 points/period, the optimal lag seems to be 24 or 26 and for 20 points/period, maximum lags 50–58 seem to offer the highest sensitivity. Positive detections from the linear redundancy statistic (bottom) indicate at which maximum lag the surrogates should not be used anymore. The curve for 5 points/period (triangles) coincides with the abscissa.

generated AR(5) and Lorenz time series. The number of experiment realizations in which the test positively detects the presence of a nonlinear component was expressed as the "detection rate." The detection rate for each maximum lag is the number of successfully detected segments (with  $p < 0.05$ ) relative to the total number of experiments for the given lag (200).

In practice the question of optimal sampling is important. If the extracted oscillatory mode is undersampled with too few points per period, not enough dynamical information is retained in the time series and the discriminatory power of the proposed procedure is expected to be low. With a sampling frequency too high, the autoregressive model fitted to the extracted mode may start adjusting itself to stochastic features in the time series and reach a very high order. The surrogates will then preserve characteristics of the signal which do not pertain to its dynamics. Clearly a balance must be struck in the sampling of the tested mode. The numerical experiment takes this into account and tests the discrimination capabilities of the method for various points-per-period samplings. The results for the detection of the Lorenz activity in the band (0.05–1.05) are summarized in Fig. 3 which shows how the detection statistics vary with the number of points per period of the central frequency (0.55). The plot results indicate that a sampling rate of 5 points/period of the central frequency does not facilitate a sensitive detection. Better results are obtained for 10 or 20 points per period. The main difference is that different lengths of linear and nonlinear regularity curves are required for optimal detection. For more points per period longer sequences are necessary. It is worth noting that the number of cycles of the central frequency for optimal detection is not changed appreciably and is slightly more than 2 cycles for both sampling rates.

As a control experiment, the strong peak at frequency around 1.7 was also tested with the same bandwidth as the Lorenz activity. The edge frequencies of the second order

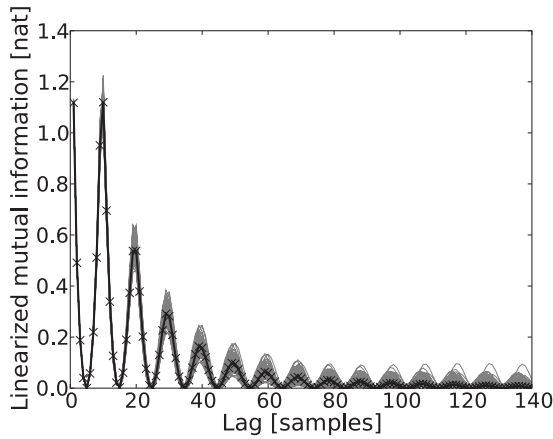


FIG. 4. Linear redundancy curves for data (thick black line) and for 50 surrogates (thin gray lines). The redundancy curve for the data segment matches the shape of the surrogate curves up to maximum lag of about 80 in this example.

Butterworth filter were set to (1.2–2.2) and filtering was performed using the forward/backward strategy. Positive detections lie always under 1% for both linear and nonlinear redundancies up to a maximum lag of 60 (results not shown). Although there is a clear peak in the power spectrum of the signal at the frequency of 1.7 and none where the Lorenz activity is concentrated, the proposed method has been able to discriminate between the embedded broadband nonlinear activity and the linearly filtered noise perfectly by confirming the nonlinear activity in the band of 0.05–1.05 and by rejecting nonlinear oscillations in the band of 1.2–2.2 around the spectral peak.

## B. Experimental data analysis

Two nights of sleep EEG were analyzed from one healthy subject to show how the method works on an experimentally obtained data set. The EEG was measured within the framework of the European Commission funded SIESTA program. Detailed description of the data and different types of their analyses can be found in Refs. 19 and 20. The sampling frequency was 256 Hz and the measured signal was filtered by a high-pass filter with frequency of 0.1 Hz and a low pass filter with frequency of 75 Hz. The recording was split into 30 s segments which have been classified into sleep stages (1–5) according to the standard Rechtschaffen and Kales<sup>21</sup> criteria.

In this work sigma band and alpha band activity were analyzed in the EEG obtained from the electrode C3 with a contralateral reference on the right mastoid. Both activities were extracted using bandpass filtering in the same manner as in the numerical example: using a forward/backward filtering strategy with a second order Butterworth filter to nullify the phase shift. The filter edge frequencies were set to 11 and 17 Hz ( $14 \pm 3$  Hz) for the sigma band and to 8 and 12 Hz for the alpha band.

The time series was subsampled so that  $\approx 9$  points/period (at the center frequency of 14 Hz) were available for the analysis of sigma band activity. Figure 4 shows the linear redundancies for a sample 30 s segment of the EEG filtered

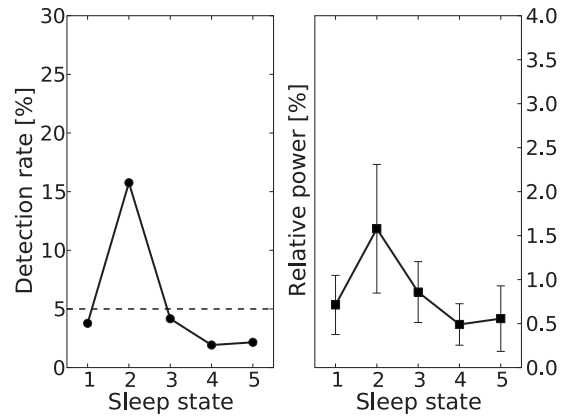


FIG. 5. Detection of nonlinear oscillations in the sigma band during the first recording night (left). The proposed method indicates the existence of nonlinear oscillations in the sigma band in the second sleep stage exclusively. Relative power of the sigma band (right) suggests the same.

in the sigma band. The surrogates replicate the linear structure accurately at least until lag 80 in the given example. Upon examination of the linear redundancy curves of several random segments, it was ascertained that maximum lags between 60 and 100 were adequate. The following analysis has been performed with maximum lags of 60 and 100. It was found that the results did not differ significantly. The length of one 30 s segment was 7680 points. The fitted autoregressive model order fluctuated between 30 and 40, rarely exceeding 40.

The detection results (number of segments with positively detected nonlinear oscillatory activity relative to the total number of segments of a particular sleep stage) for the first night are shown in Figs. 5 and 6. The nonlinear oscillatory activity in the sigma band was detected only in the second sleep stage. The relative power of the sigma band seems to agree well with these results. In the alpha band, the proposed detection method has not indicated any consistent nonlinear oscillations, whereas the relative power statistic supports the claim that alpha band activity exists in the second sleep stage and in the fifth sleep stage, REM sleep (rapid eye movement).

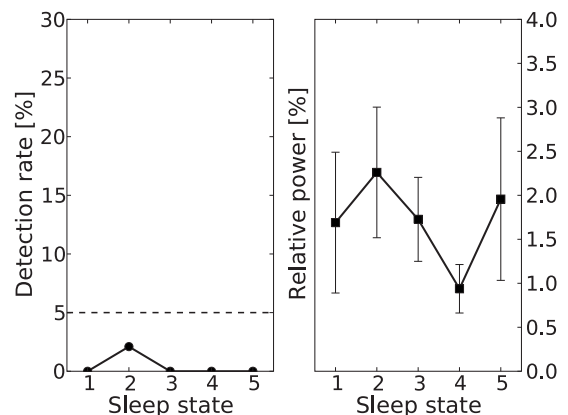


FIG. 6. Detection of nonlinear oscillations in the alpha band during the first recording night (left). The proposed method has not detected any consistent nonlinear oscillatory activity. The relative power (right), however, suggests that alpha activity is increased in sleep stage 2 and in REM sleep.

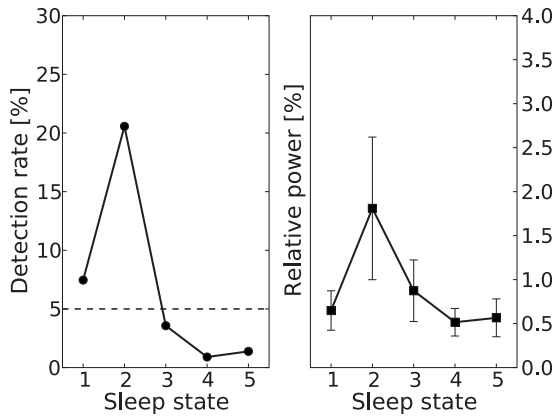


FIG. 7. Detection of nonlinear oscillations in the sigma band during the second recording night (left) and related relative power in the sigma band (right). Nonlinear oscillations have been detected in the second sleep stage and sparsely during the first sleep stage. Sigma band power seems to suggest a similar activity pattern.

Figures 7 and 8 show the results for the second analyzed night of the same person. The proposed method has identified clear nonlinear oscillations in the sigma band in the second sleep stage. Additionally in the first sleep stage, some segments have been marked as containing nonlinear sigma band activity. The portion of significant windows is very low ( $\approx 7.5\%$ ) compared to the nominal significance level of the test (5%). The detected segments could be a result of a statistical fluctuation or could indicate that a small amount of segments contain low amplitude sigma activity not visually perceptible in the broadband signal. The relative power plot seems to indicate that sigma activity should be expected in the second sleep stage. For the alpha band the previous situation is reiterated: the proposed method does not give a clear indication of nonlinear oscillations in the alpha band in any sleep stage but relative power statistics indicate a proliferation of alpha band activity in multiple stages (sleep stage 1, 2, and REM sleep—stage 5). According to the Rechtschaffen and Kales criteria, some alpha band activity may exist in the first sleep stage.

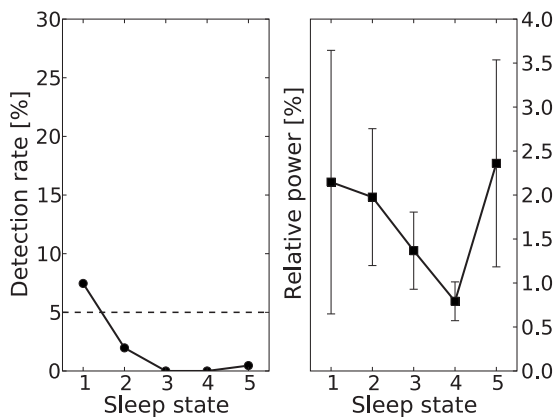


FIG. 8. Detection of nonlinear oscillations in the alpha band during the second recording night (left) and related relative power in the alpha band (right). Some positive detections exist in the first sleep stage. Relative alpha band power fluctuates strongly inside the sleep stages and is increased in stages 1, 2, and 5.

#### IV. DISCUSSION AND CONCLUSION

The proposed method attempts to identify consistent nonlinear oscillatory activity inside a part of a broadband signal. Frequently parts of broadband signal are extracted using several available methods such as bandpass filtering, wavelet convolution, EMD, or SSA decomposition. The focus of this work is a method to statistically test if such an extracted mode can be assumed to have been generated by a nonlinear process. This is important because even filtered noise seems to have an oscillatory character, and it is often misleading to suppose that the narrow-band signal is a result of an oscillatory activity generated by some underlying nonlinear dynamics. The test is constructed using the method of surrogate time series which are generated using an autoregressive model fit to the data. A visual examination and a linear redundancy index are employed to verify whether the surrogate time series match the linear structure of the original data sufficiently well and under which conditions such as sampling rate (points per period) and maximum lag. This information is then used to construct a test of nonlinearity for a particular mode. If the nonlinear redundancy index can be used to reject the hypothesis that the generating system is linear, then it is inferred that a nonlinear process was involved in the generation of the analyzed activity and the activity is consistent inside some analyzed time segment.

The motivation and purpose of the presented method is fundamentally different from previously introduced method to detect particular activity types. The method introduced by Olbrich *et al.*<sup>22,23</sup> analyzes the shape of the broadband EEG signal (without narrow-band filtering) and identifies short-lived activity by fitting an autoregressive model to a short window and analyzing the model properties (frequency and damping). This is an accurate determination of the existence of oscillatory activity. However, the type of oscillatory activity is not the main issue. Additionally short-lived activity such as clear sleep spindles can be detected by the method.

Another approach advocated by Chavez *et al.*<sup>24</sup> is aimed at testing whether the instantaneous phase extracted from a mode satisfies the conditions that are assumed to hold for the phase. The authors use thresholds to determine whether the variations in amplitude are slow enough with respect to the change in the phase. This method examines the inherent variability in the phase and amplitude and is thus another approach different from both that of Olbrich *et al.* and of the proposed method.

The method suggested in this work focuses on activity that is of longer duration and can be attributed to a source with nonlinear dynamics but may be difficult to detect without prior extraction. A positive detection using our method supports further analysis using phase dynamics. A negative statement can help identify signals where it might be futile to attempt to detect synchronization or directional influence using the phase dynamics approach for lack of acceptable nonlinear oscillatory activity. In such cases the standard linear coherence analysis is preferred.

The method has been shown to work on a numerical example which mixed the  $x$ -component of the Lorenz oscillator with a fifth order autoregressive process. The method has detected the nonlinear signal in the low frequency range.

On the other hand, a clear peak in the spectrum of the signal which arose by a filtering of white noise (by the autoregressive process itself) has not been identified as having nonlinear content. This experiment has shown that rather than being sensitive to the shape of the signal, the method is sensitive to the type of dynamics that generated the signal. It has been demonstrated that nonlinear oscillatory activity need not be associated with a spectral peak and conversely a spectral peak need not indicate that phase dynamics can be applied to the corresponding oscillatory mode.

Experimental data in the form of EEG from a sleeping subject are analyzed and the findings are shown to conform to the expected results based on the criteria of Rechtschaffen and Kales<sup>21</sup> for sleep stage classification. Sleep stage 2, characterized by the existence of sigma activity, has been identified as containing nonlinear oscillatory components. This supports the claim that phase dynamics can be applied to entire EEG segments measured in the second sleep stage as the existence of a consistent nonlinear activity can be assumed. Relative power also indicates a similar tendency for the sigma activity. In the alpha band, the proposed method gives results consistent with the Rechtschaffen and Kales criteria stating no oscillatory phenomena in the alpha band during sleep, although the relative power indicates alpha band activity in three of the five sleep stages.

The proposed method is promising for identification of nonlinear oscillatory processes embedded or hidden in a broadband noisy background. Such problems frequently arise in neurophysiology when analyzing signals recorded on various levels of organization of brain tissues, as well as in other fields when possibly interacting and synchronizing oscillations, emerge in complex dynamical processes.

## ACKNOWLEDGMENTS

The authors would like to acknowledge the Siesta Group Schlafanalyse GmbH as the source of the sleep EEG and thank them for making their data available. We would also

like to thank Kristína Šušmáková for helpful discussions about the sleep EEG. This work has been supported by the EC FP7 project BrainSync (Grant No. HEALTH-F2-2008-200728) and in part by the Institutional Research Plan Grant No. AV0Z10300504.

<sup>1</sup>G. Buzsáki and A. Draguhn, *Science* **304**, 1926 (2004).

<sup>2</sup>L. M. Ward, *Trends Cogn. Sci.* **7**, 553 (2003).

<sup>3</sup>P. Bob, M. Paluš, M. Šušta, and K. Glaslová, *Neurosci. Lett.* **447**, 73 (2008).

<sup>4</sup>E. Basar and B. Güntekin, *Brain Res.* **1235**, 172 (2008).

<sup>5</sup>A. Pikovsky, M. Rosenblum, and J. Kurths, *Synchronization: A Universal Concept in Nonlinear Sciences*, Cambridge Nonlinear Science Series (Cambridge University Press, Cambridge, 2003).

<sup>6</sup>M. Paluš and A. Stefanovska, *Phys. Rev. E* **67**, 055201 (2003).

<sup>7</sup>R. Vautard and M. Ghil, *Physica D* **35**, 395 (1989).

<sup>8</sup>M. R. Allen and L. A. Smith, *Phys. Lett. A* **234**, 419 (1997).

<sup>9</sup>M. Paluš and D. Novotná, *Nonlinear Processes Geophys.* **11**, 721 (2004).

<sup>10</sup>M. Paluš and D. Novotná, *J. Atmos. Sol.-Terr. Phys.* **69**, 2405 (2007).

<sup>11</sup>J. Theiler, S. Eubank, A. Longtin, B. Galdrikian, and J. D. Farmer, *Physica D* **58**, 77 (1992).

<sup>12</sup>T. Schreiber and A. Schmitz, *Physica D* **142**, 346 (2000).

<sup>13</sup>J. Theiler and D. Prichard, *Physica D* **94**, 221 (1996).

<sup>14</sup>D. Kugiumtzis, *Stud. Nonlinear Dyn. Econometrics* **12**, 4 (2008).

<sup>15</sup>J. Theiler, P. S. Linsay, and D. M. Rubin, *Santa Fe Institute Studies in the Sciences of Complexity*, edited by A. S. Weigend and N. A. Gershenfeld (Addison-Wesley, Reading, MA, 1993), Vol. XV, p. 429.

<sup>16</sup>M. Paluš, *Physica D* **80**, 186 (1995).

<sup>17</sup>G. Schwarz, *Ann. Stat.* **6**, 461 (1978).

<sup>18</sup>M. Paluš and M. Vejmelka, *Phys. Rev. E* **75**, 056211 (2007).

<sup>19</sup>P. Anderer, G. Gruber, S. Parapatics, M. Woertz, T. Miazhyńska, G. Klosch, B. Saletu, J. Zeithofer, M. J. Barbanoj, H. Danker-Hopfe, S. L. Himanen, B. Kemp, T. Penzel, M. Grozinger, D. Kunz, P. Rappelsberger, A. Schlogl, and G. Dorffner, *Neuropsychobiology* **51**, 115 (2005).

<sup>20</sup>K. Šušmáková and A. Krakovská, *Artif. Intell. Med.* **44**, 261 (2008).

<sup>21</sup>A. Rechtschaffen and A. Kales, *A Manual of Standardized Terminology, Techniques, and Scoring Systems for Sleep Stages of Human Subjects* (U.S. Department of Health, Education and Welfare, National Institutes of Health, Bethesda, MD, 1968).

<sup>22</sup>E. Olbrich, P. Achermann, and P. Meier, *Neurocomputing* **52–54**, 857 (2003).

<sup>23</sup>E. Olbrich and P. Achermann, *Neurocomputing* **58–60**, 129 (2004).

<sup>24</sup>M. Chavez, M. Besserve, C. Adam, and J. Martinerie, *J. Neurosci. Methods* **154**, 149 (2006).